MDPI

Article

Mixed-Effects Height Prediction Model for *Juniperus procera* Trees from a Dry Afromontane Forest in Ethiopia

Mindaye Teshome [1,2], Evaldo Muñoz Braz [3], Carlos Moreira Miquelino Eleto Torres [1], Dimitrios Ioannis Raptis [4], Patricia Povoa de Mattos [3], Hailemariam Temesgen [5,*], Ernesto Alonso Rubio-Camacho [6] and Gudeta Woldesemayat Sileshi [7]

1 Departamento de Engenharia Florestal, Universidade Federal de Viçosa (UFV), Viçosa 36570-900, MG, Brazil; mindaye.legese@ufv.br (M.T.)
2 Ethiopian Forestry Development, P.O. Box 24536, Addis Ababa 1000, Ethiopia
3 Embrapa Florestas, Estrada de Ribeira, Km 111 sn Guaraituba C.P: 319, Colombo 83411-000, PR, Brazil; evaldo.braz@embrapa.br (E.M.B.); patricia.mattos@embrapa.br (P.P.d.M.)
4 Department of Forestry and Natural Environment, International Hellenic University, 1st Km Drama-Mikrohori, 66100 Drama, Greece
5 Department of Forest Engineering, Resources, and Management, College of Forestry, Oregon State University, Corvallis, OR 97331-5704, USA
6 Instituto Nacional de Investigaciones Forestales, Agrícolas y Pecuarias, Centro de Investigación Regional Pacífico Centro, Av. Biodiversidad 2470, Tepatitlán de Morelos 47600, Jalisco, Mexico; ernestorub@gmail.com
7 Department of Plant Biology and Biodiversity Management, Addis Ababa University, Addis Ababa P.O. Box 1176, Ethiopia; sileshigw@gmail.com
* Correspondence: hailemariam.temesgen@oregonstate.edu

Abstract: Tree height is a crucial variable in forestry science. In the current study, an accurate height prediction model for *Juniperus procera* Hochst. ex Endl. trees were developed, using a nonlinear mixed-effects modeling approach on 1215 observations from 101 randomly established plots in the Chilimo Dry Afromontane Forest in Ethiopia. After comparing 14 nonlinear models, the most appropriate base model was selected and expanded as a mixed-effects model, using the sample plot as a grouping factor, and adding stand-level variables to increase the model's prediction ability. Using a completely independent dataset of observations, the best sampling alternative for calibration was determined using goodness-of-fit criteria. Our findings revealed that the Michaelis–Menten model outperformed the other models, while the expansion to the mixed-effects model significantly improved the height prediction. On the other hand, incorporating the quadratic mean diameter and the stem density slightly improved the model's prediction ability. The fixed-effects of the selected model can also be used to predict the mean height of *Juniperus procera* trees as a marginal solution. The calibration response revealed that a systematic selection of the three largest-diameter trees at the plot level is the most effective for random effect estimation across new plots or stands.

Keywords: forest inventory; native tree; allometry; calibration; stand volume; *Juniperus procera*

1. Introduction

Tree height is a crucial variable for determining the aboveground biomass, volume, site productivity, and the vertical structure of forest stands [1–5]. However, direct tree height measurement can be challenging, especially for tall tropical tree species with irregular crowns [6–8]. The observed difficulty can be effectively addressed by developing height–diameter models [9].

Earlier studies suggested that height–diameter relationships vary among tree species, stands, and geographic regions [10–13]. However, recent evidence indicates that much of the variability arises from measurement errors, sampling biases, and failure to capture the diameter size distribution [14]. They found out that plants exhibit a striking similarity in allometry across taxonomic lineages, climate zones, biomes, and disturbance regimes [14].

Therefore, it becomes very crucial to employ larger sample sizes and ensure that samples are representatives of the size-frequency distribution of the target population when developing height–diameter models. Various studies also reported that using additional predictors like basal area, density, dominant height, and quadratic mean diameter can improve prediction accuracy without requiring separate models for each stand [15–18]. Hence, explicitly accounting for the methodological artifacts and the ecological drivers will be very important to developing a precise height prediction model.

The basic data used for developing height prediction models typically come from randomly established sample plots within a forest stand. Such data have a clustered structure, with trees grouped within plots, leading to correlated observations [19]. Fitting a model to correlated data through the ordinary least squares (OLS) method may lead to biased estimation of the confidence intervals for the model parameters [20]. Mixed-effects modeling approaches are better suited for clustered data, accounting for the lack of independence and incorporating height–diameter variability across forest types, locations, plots, and species that fixed-effects models do not consider. Mixed-effects models estimate both fixed and random effects related to individual subjects (e.g., sample plots), simultaneously modeling both fixed-effects and subject-specific parameters [21]. Recent studies have demonstrated that mixed-effects models outperformed fixed-effects models for height predictions using data collected through a plot sampling approach by accounting for data structure and lack of independence between observations [9,15,16,22]. However, the prediction performance of these models in our specific study area remains uncertain.

Until now, few attempts have been made to develop robust height prediction models for Afromontane tree species, while numerous models exist for different tree species in temperate (e.g., [15,23–26]) as well as tropical forests [10,27–31]. In Ethiopia, the existing models are limited in scope and geographic applicability [32–34]. Hence, developing an accurate height prediction model for *Juniperus procera*, an ecologically and economically valuable tree species, would improve biomass and carbon stock estimation from Afromontane forests.

In this study, we developed a robust height prediction model for *Juniperus procera* Hochst. ex Endl. trees from the Chilimo Dry Afromontane Forest in Ethiopia. The objectives of the study were to (1) assess the prediction performance of various local models and select the best model; (2) develop a mixed-effects model to analyze plot-level predictions; (3) evaluate the contribution of additional stand variables on predictions; and (4) determine the optimal sampling alternative for calibrating the best model. The developed model provides an efficient means of estimating *Juniperus procera* tree height in situations where direct measurements are lacking.

2. Materials and methods

2.1. Study Area

The data used in this study were collected from the Chilimo and Menagesha Suba Dry Afromontane Forests (Figure 1). The Chilimo Forest is geographically located from 38°05′ to 38°15′ E and 9°00′ to 10°10′ N, at an altitudinal range of 1700–3200 m [35]. The area experiences a unimodal pattern of rainfall distribution that occurs from May to November, with July having the highest peak. The mean annual temperature ranges between 15 and 20 °C, and its average annual precipitation ranges between 1000 and 1264 mm [35]. The major soil types around the study areas are Vertisols, Luvisols, and Cambisols [36]. The soils are reddish-brown, gravelly, and shallow at higher altitudes, while at lower sites, they tend to become dark gray and deep [36,37]. According to Mammo and Kebin [38], the surface soil (0–20 cm) in the Chilimo Forest has higher levels of total nitrogen, available phosphorus, potassium, and a higher percentage of organic matter. The calibration dataset was collected from the Menagesha Suba Dry Afromontane Forest. The Menagesha Suba Forest is located between 38°31′30″ E and 38°34′30″ E to 8°57′0″ N and 9°0′ N, with an altitude ranging between 2200 and 3385 m [39]. The area receives on average 1056 mm of rainfall per year, and the average monthly temperature ranges from 6 to 22 °C. The

rainfall pattern is bimodal, with a long rainy season from June to September and a short rainy season between April and May [40]. The data collected from the Menagesha suba Dry Afromontane Forest was used for calibration.
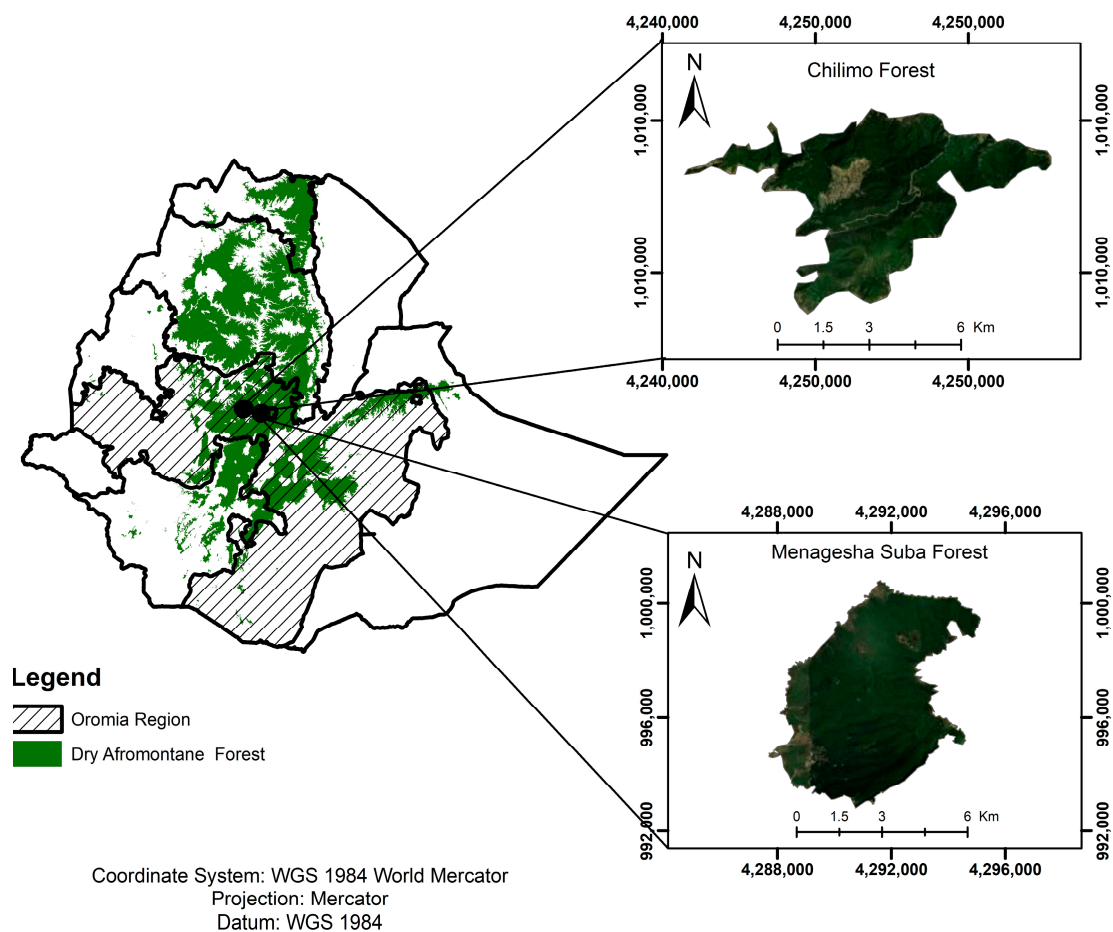

Figure 1. Map of the study area overlaid with the distribution map of dry Afromontane forests, following Friis et al. [41].

2.2. Data Collection

For the needs of the current research, forest inventory studies were conducted in the Chilimo and Menagesha Suba forests, in 2018. A total of 131 sample plots (20 m × 20 m) were established along transect lines. The first transect was aligned parallel to the edge of the forest, and others were laid out at 500 m intervals along the transect lines [42,43]. The first sample plot was located randomly, and the subsequent plots were established at 300 m intervals. In each sample plot, the diameter at breast height (dbh) and total height (ht) of all trees with dbh $\geq$ 2.0 cm were measured using a diameter tape and a Vertex IV ultrasonic hypsometer (Haglöf Sweden AB, Långsele, Sweden). The local names of all trees were recorded and identified to the species level in the field, following the *Flora of Ethiopia and Eritrea* [44–48]. For those species that were difficult to identify in the field, their specimens were collected, pressed, and identified at the National Herbarium, Addis Ababa University. The data were used to compute the quadratic mean diameter (Dq), basal area (G), dominant height (hd) (the average height of the 100 tallest trees per hectare), dominant diameter (Dd) (the diameter for the average height of the 100 tallest trees per hectare), and the number of trees per hectare (N).

2.3. Juniperus procera Hochst. ex. Endl.

We chose *Juniperus procera* Hochst. ex. Endl., commonly known as the "African Pencil Cedar," as the main species for this study because of its value as a native timber tree. It is an evergreen coniferous tree that occurs predominantly in the dry Afromontane forests, mainly between 1500 and 3000 m. It grows to a height of 40 m and a diameter of 3 m [49,50]. This species was once regarded as threatened in the IUCN red list (in 2011) but has since been assessed as a species of least concern [51]. Its native range covers Congo, the Democratic Republic of Congo, Djibouti, Eritrea, Ethiopia, Kenya, Malawi, Saudi Arabia, Somalia, Sudan, Tanzania, Uganda, Yemen, and Zimbabwe [52]. It is grown in plantations in its native range and elsewhere, including South Africa, France, the United Kingdom, the United States, India, and Australia for timber production and environmental protection [52]. Wood is resistant to decay and termite attacks and is used for various purposes. It is also a valuable timber tree species in the East African highlands and is the most preferred tree in Ethiopia [53]. It is adapted to high-elevation climates with low precipitation characteristics of Afromontane forests, which constitute a unique forest type occurring on high African mountains [50,54]. The diameter and height data of *Juniperus procera* trees were extracted from the data collected in the 2018 forest inventory in the Chilimo and Menagesha Suba forests and used to develop a height prediction model. Descriptions of the dataset are presented in Table 1.

Table 1. Summary statistics of the fitting and calibration datasets.

Variables	Fitting Dataset—Chilimo Forest				Calibration Dataset—Menagesha Suba Forest			
	Mean	**Min.**	**Max.**	**Std**	**Mean**	**Min.**	**Max.**	**Std**
dbh	21.10	2.00	121.20	18.45	14.3	2.0	71.0	12.7
ht	13.55	2.00	43.22	7.76	9.9	1.6	28.0	6.2
G	11.27	0.01	87.60	15.89	2.0	0.01	16.9	4.4
N	484.48	25.00	2750	773.37	606.8	21.0	1149	365.8
hd	10.71	2.00	38.67	6.77	4.6	1.4	14	2.5
Dd	18.47	2.53	71.70	13.12	9.1	2.0	25.9	6.5
Dq	16.23	2.00	79.80	13.81	5.4	2.0	23.9	6.1
Total sample	*n* = 1215 trees from 101 rectangular plots				*n* = 300 trees from 30 rectangular plots			

Note: dbh = diameter at breast height (cm), ht = total height (m), N = stand density (trees ha^{-1}), G = basal area (m^2 ha^{-1}), Dq = quadratic mean diameter (cm), hd = dominant height (m), Dd = dominant diameter (cm), Min = minimum, Max = maximum, and Std = standard deviation.

2.4. Statistical Analysis

2.4.1. Base Model Selection

The relationship between tree height and stem diameter has been described using a variety of mathematical functions, and several nonlinear model forms have been statistically tested to describe the allometry behind this complex relationship (e.g., [9,55,56]). Some models are grounded in sound theory, while others are purely empirical. The power law function is the most common model, based on many theoretical arguments [14]. Mehtatalo and Lappi [57] suggested that flexibility and parsimony (i.e., combining simplicity with high predictive or explanatory power) should be considered in addition to the parameter's obvious biological interpretability when choosing the best function. For the needs of the current study, we evaluated 14 local nonlinear functions (Table 2) that have been widely used to describe the height–diameter relationships of trees from both plantation and natural forests growing in different regions [15,28,58–60], and the best model was referred to as the base model.

The fitting procedure of the local models in the Chilimo dataset (Table 1) was based on the generalized least squares technique (GLS), through the *gnls* function in R software version 3.6.0 [61]. The model's prediction bias, the root mean square error (RMSE), the Akaike information criterion (AIC) (Equations (1)–(3)), and graphical analysis were used to compare the predictive performance of the models and select the best-fitted model [16].

Table 2. Lists of candidate equations for height modeling.

No	Name	Mathematical Expression	References
M1	Power	$ht = 1.3 + \beta_0 \times dbh^{\beta_1}$	[62]
M2	Näslund	$ht = 1.3 + \dfrac{dbh^2}{(\beta_0 + \beta_1 \times dbh)^2}$	[63]
M3	Curtis	$ht = 1.3 + \dfrac{\beta_0 \times dbh}{(1 + dbh)^{\beta_1}}$	[18]
M4	Meyer	$ht = 1.3 + \beta_0(1 - exp(-\beta_1 \times dbh))$	[64]
M5	Schumacher	$ht = 1.3 + \beta_0 exp(-(\beta_1/dbh))$	[65]
M6	Michaelis–Menten	$ht = 1.3 + \beta_0 \times dbh/(\beta_1 + dbh)$	[66]
M7	Gomperz	$ht = 1.3 + \beta_0 exp(-\beta_1 exp(-\beta_2 \times dbh))$	[67]
M8	Logistic	$ht = 1.3 + \dfrac{\beta_0}{1 + \beta_1 exp(-\beta_2 \times dbh)}$	[56]
M9	Chapman–Richards	$ht = 1.3 + \beta_0(1 - exp(-\beta_1 \times dbh))^{\beta_2}$	[68,69]
M10	Weibull	$ht = 1.3 + \beta_0\left(1 - exp\left(-\beta_1 \times dbh^{\beta_2}\right)\right)$	[70]
M11	Lundqvist Korf	$ht = 1.3 + \beta_0 exp\left(-\beta_1 \times dbh^{\beta_2}\right)$	[62]
M12	Ratkowsky	$ht = 1.3 + \beta_0 exp(\beta_1/dbh + \beta_2)$	[71]
M13	Hossfeld IV	$ht = 1.3 + \beta_0/\left[1 + \left(\dfrac{1}{\beta_1 \times dbh^{\beta_2}}\right)\right]$	[62]
M14	Johnson–Schumacher	$ht = 1.3 + \beta_0 exp(-\beta_1/dbh + \beta_2)$	[62]

Note: dbh = over bark diameter at breast height in cm, ht = total tree height in m; β_0, β_1, and β_2 are parameters of the height–diameter models.

The following power-type variance function (var(e) = $\sigma^2 |dbh|^{2\delta}$) was also applied to correct the observed heteroscedasticity in the residuals of all models:

$$\text{Bias} = \frac{\sum_{i=1}^{n}(y_i - \hat{y}_i)}{n} \qquad (1)$$

$$\text{RMSE} = \sqrt{\frac{\sum_{i=1}^{n}(y_i - \hat{y}_i)^2}{n - p}} \qquad (2)$$

$$\text{AIC} = n\,log\left(\frac{SSR}{n}\right) + 2p \qquad (3)$$

where y_i = measured height, y_i = predicted height, $\hat{y}_i$ = average, n = total number of height measurements, p = number of parameters of the equation, and SSR = sum of the squares of the residuals; RMSE = root mean square of error; and AIC = Akaike information criterion.

A rank was assigned to the fit statistical values of each model [72]. Then, these ranks were aggregated by adding them to calculate each model's final fit rank. This ranking system indicates the model's performance concerning all the considered fit statistics criteria. Furthermore, the models' compliance with the constant variance assumption was also examined by plotting the residuals against the standardized diameter. The mywhiskers function in the R package *lmfor* was utilized to plot the means of residuals in 10 relative diameters classes, together with the confidence intervals for individual observation (mean ± 1.96 SD) and the 95% confidence intervals for the class mean, to detect the potential heteroscedasticity in the residuals [9,15]. The difference between each tree's diameter and the plot's mean diameter, divided by the diameter's standard deviation, was used to calculate standardized diameters [9]. Finally, the parameters of the best-fitted model were obtained by fitting the model with the entire dataset.

2.4.2. Nonlinear Mixed-Effects Modeling

Once the best generalized nonlinear least squares model was selected, we proceeded to expand the parameters with random effects. At this stage, we used a subject-specific

nonlinear mixed effects model (NLMEM) due to the hierarchical structure of the data, i.e., trees within plots. Several relevant studies have shown that observations from the same sampling unit are highly correlated (e.g., [12,20,73]). This indicates a clear violation of the fundamental least squares assumption, wherein observations are expected to be independent, and biased confidence intervals of the mean value of the parameters are expected. To deal with this problem, earlier studies proposed a nonlinear mixed-effects modeling approach [9,12,15,16]. The random-effects parameters describe a particular cluster (sample plot), while the fixed-effects parameters reflect the population average of the data [74]. More recently, NLMEMs have been widely applied in modeling height–diameter relationships [26,30,59,75–77]. The parameters were estimated using the "nlme" library [78] in R software version 3.6.0 [61]. This allows for comparing the different nested mixed-effects model forms (Table 3) and the selected base model by the ANOVA function to test the significance, including random effects, as both models have the same fixed effects. Model evaluation was performed using the goodness of fit criteria, such as RMSE, bias, and AIC values.

Table 3. The evaluated nonlinear mixed-effects models with different random-effects structures.

No.	Model Forms	Random Effects
M1	$\mathrm{ht} = 1.3 + (\beta_0 + u_{0i}) \times \mathrm{dbh}/((\beta_1 + u_{1i}) + \mathrm{dbh})$	The random effect at β_0 and β_1
M2	$\mathrm{ht} = 1.3 + (\beta_0 + u_{0i}) \times \mathrm{dbh}/(\beta_1 + \mathrm{dbh})$	The random effect at β_0
M3	$\mathrm{ht} = 1.3 + \beta_0 \times \mathrm{dbh}/((\beta_1 + u_{1i}) + \mathrm{dbh})$	The random effect at β_1

Note: ht is the height, dbh is the diameter at breast height of the tree, β_0 and β_1 are the fixed effects parameters, and the u_i indicates the estimated random effects.

2.4.3. Generalized Mixed-Effects Models

The contribution of estimated stand variables (Table 1) was also evaluated to improve the predictive performance of the best simple mixed-effect model. First, we conducted correlation analysis to assess the relationship of the stand variables with the parameters of the best mixed-effects model. During the analysis, different combinations of the selected stand variables were entered as predictors in the model and the fitting performances were evaluated using the RMSE, the prediction bias, and the corresponding AIC values. Then, a generalized mixed-effects model was developed using the most highly correlated stand predictor variables.

2.4.4. Calibration and Random Effect Estimation

Two different types of predictions can be accomplished using the mixed-effects modeling approach [9,79]. The first is a fixed effect or marginal prediction, which offers predictions using only the fixed part of the model. The second is conditional prediction, which provides a more accurate prediction for a given sample plot because it uses both the model's random and fixed elements to make tree height predictions. However, when height measurements are available from subsampled trees, it is possible to localize the random effects to a new plot; this process is also known as localization. In this study, we used localization to determine the plot-specific random effects, and to evaluate the model's performance [9,15,79]. Based on the subsample data, random effects $\hat{b}_i$ was predicted using the following equation [80]:

$$\hat{b} = \hat{D}\hat{Z}_i^T \left(\hat{R}_i + \hat{Z}_i\hat{D}\hat{Z}_i^T \right)^{-1} \hat{e}_i$$

where $\hat{D}$ is the estimated variance–covariance matrix associated with the random effects at the plot level, $\hat{R}_i$ is the estimated variance–covariance matrix for the error term, $\hat{Z}_i$ is the partial derivatives matrix concerning the random effects, and $\hat{e}_i$ is the error matrix estimated using the fixed parameters only.

The detailed procedure for the random effects parameter estimation using a nonlinear mixed-effects modeling approach was presented by Calama and Montero [12]. The calibration response of the best local mixed-effect and generalized mixed-effects models was assessed using a completely independent dataset from the Menagesha Suba Dry Afromontane Forest (Table 1). Overall, nine different sampling alternatives (Table 4) were evaluated, and the best sample size (the number of trees) and method were identified, following the procedure in Camacho et al. [81]. We evaluated the effectiveness of the sampling alternatives for estimating the random effects by examining the root mean square error (RMSE) values and contrasting them with the RMSE estimates obtained from using the best local mixed-effects and generalized mixed-effects models, which consider all the trees within the sample plot.

Table 4. The evaluated sampling alternatives for calibration response.

Code	Sampling Alternatives
A1.	Utilizing measurements from selected trees with diameters near the quartiles (the 25th, 50th, and 75th percentiles) of the diameter distribution.
A2.	Utilizing measurements from selected trees with diameters close to the first and the second quartiles (25th and 50th percentiles) of the diameter distribution
A3.	Utilizing measurements from selected trees with diameters close to the first and the third quartiles (25th and 75th percentiles) of the diameter distribution
A4.	Utilizing measurements from selected trees with diameters close to the second and the third quartiles (50th and 75th percentiles) of the diameter distribution
A5.	Utilizing measurements from selected trees with diameters close to the second quartile (50th percentile) of the diameter distribution
A6.	Utilizing measurements from selected trees with diameters close to the quadratic mean diameter (Dq), the smallest diameter (*dmin*), and the largest diameter trees (*dmax*) in each sample plot
A7.	Utilizing measurements from the smallest diameter trees (*dmin*) in each sample plot
A8.	Utilizing measurements from 1–10 randomly selected trees in each sample plot
A9.	Utilizing measurements from 1–10 systematically selected largest diameter trees in each sample plot

3. Results

3.1. Base Model Selection

The evaluated models exhibited variations in their capacity to predict the height of *Juniperus procera* trees (Table 5) in the Chilimo dataset. Among the three-parameter models, the Hossfeld IV (M13) and Chapman–Richards (M9) models, which displayed the lowest goodness-of-fit statistics values, were the most effective. Similarly, the Michaelis–Menten model (M6), with the lowest goodness-of-fit statistics values, demonstrated superior prediction performance among the two-parameter models. Furthermore, the estimated parameters of the evaluated local models were significantly different from zero at a 5% significance level.

Figure 2a–c illustrates diagnostic graphs for the Michaelis–Menten model. In Figure 2a, the average model fitting to the height–diameter data from the *Juniperus procera* tree can be observed, representing the population average curve. The observed and predicted graph (Figure 2b) demonstrates that the model makes a close prediction of the observed height. Furthermore, according to Figure 2c, no visual signs of unequal error variance can be observed, and the homoscedasticity assumption holds. The residuals are randomly distributed around the zero line, and there is no discernable systematic trend in their distribution. The thorough analysis of the diagnostics graph and the goodness-of-fit statistical values showed that the two-parameter Michaelis–Menten model (M6) outperformed the best three-parameter models. Consequently, the Michaelis–Menten model was selected as a base model for further analysis. Additional diagnostic graphs for the evaluated models can be found in the appendices (Supplementary Materials Figures S2–S4).

Table 5. Parameter estimates and fit statistical values for the local models.

Models	Parameters			Fit Statistics						Rank	
	β_0	β_1	β_2	Bias	Rank	RMSE	Rank	AIC	Rank	$\sum$	Final
M1	1.802 *	0.659 *		0.00	1	4.39	12	6398.13	11	24	8
M2	1.346 *	0.195 *		0.35	12	4.32	11	6389.49	9	32	11
M3	20.891 *	8.041 *		0.85	13	4.77	13	6531.36	13	39	13
M4	24.905 *	0.043 *		0.10	7	4.17	5	6322.19	6	18	6
M5	19.99 *	7.102 *		0.97	14	4.91	14	6586.78	14	42	14
M6	36.437 *	32.113 *		0.09	6	4.16	1	6314.99	2	9	1
M7	22.083 *	2.415 *	0.089 *	0.16	10	4.24	9	6396.07	10	29	10
M8	21.152 *	6.891 *	0.141 *	0.23	11	4.31	10	6462.61	12	33	12
M9	26.816 *	0.034 *	0.914 *	0.08	3	4.16	2	6318.97	5	10	3
M10	27.406 *	0.044 *	0.929 *	0.08	3	4.16	3	6318.42	4	10	4
M11	98.175 *	4.849 *	−0.302 *	0.08	5	4.18	8	6310.83	1	14	5
M12	31.394 *	20.392 *	5.819 *	0.12	9	4.18	7	6335.11	8	24	9
M13	36.768 *	0.031 *	−0.995 *	0.08	2	4.17	4	6316.97	3	9	2
M14	33.337 *	20.893 *	7.296 *	0.11	8	4.17	6	6329.15	7	21	7

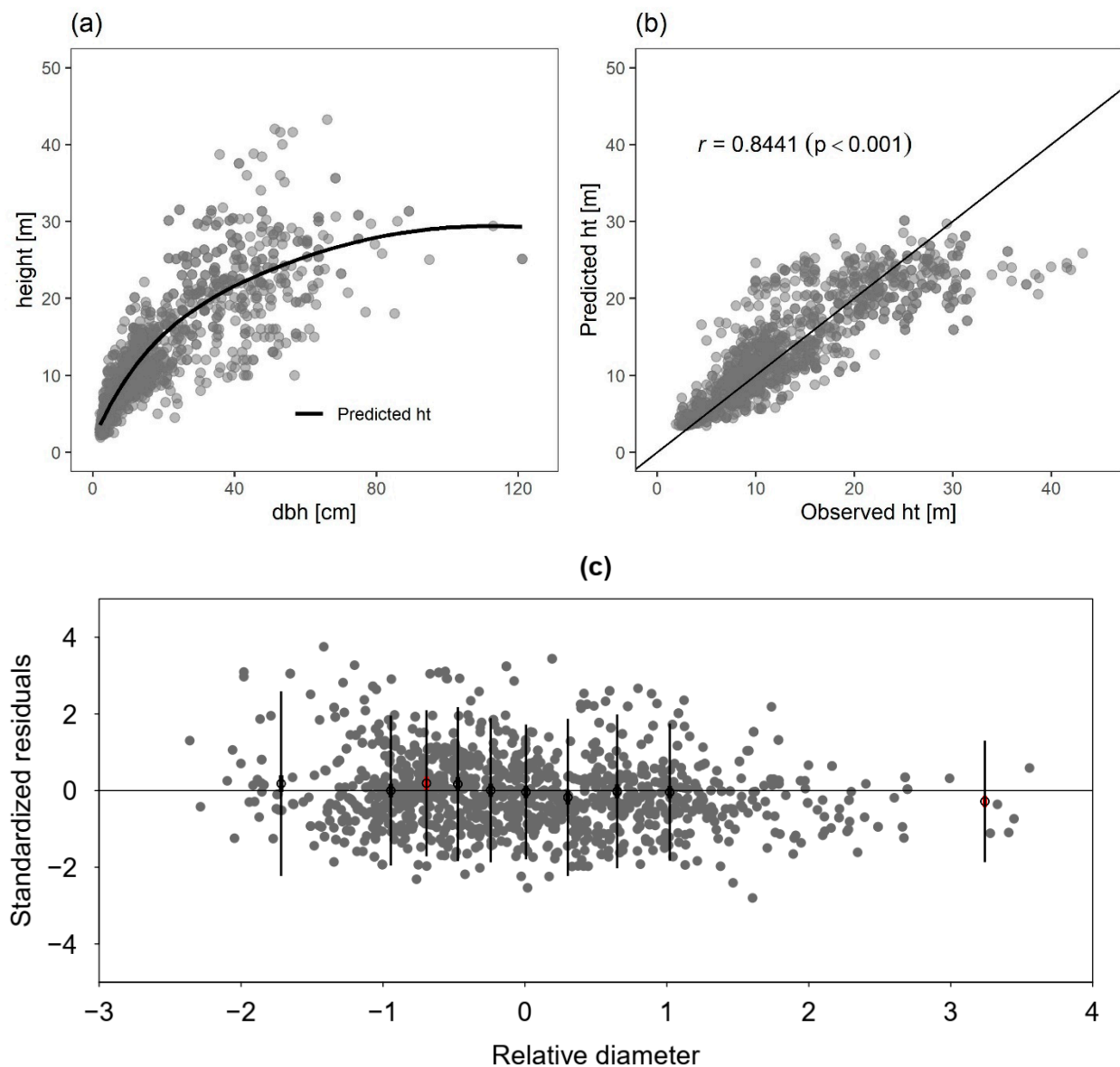Note: * indicate significant parameter estimates at $\alpha = 0.05$.

Figure 2. Height and diameter relationship (**a**), observed versus predicted height (**b**), and the residuals distribution graphs (**c**) of *Juniperus procera* trees using the Michaelis–Menten model. The gray dots in

(**a**) represent the observed height–diameter data, and the line represents the average population curve. The grey dots in (**c**) show the standardized residuals; the empty circles show the means of residuals of the diameter classes. The thin vertical lines show the confidence interval of each observation, and the thick vertical lines show the 95% confidence interval for the class mean. The thick lines that do not cross the horizontal line at $y = 0$ are highlighted in red.

3.2. Nonlinear Mixed-Effects Model

The addition of a plot-level random effect significantly enhanced the height prediction performance compared to the base model (Table 6). Through model comparison using the likelihood ratio (LTR) test, it was revealed that the mixed-effects model form with random effects on β0 and β1 (M1) displayed superior height prediction performance (L = −3114.98, df = 6, $p < 0.0001$) in comparison to the other mixed-effects model forms. Overall, the root mean square error (RMSE) values decreased from 4.16 m in the base model (Table 5) to 2.69 m in M1 (Table 6). The bias similarly decreased from 0.09 to 0.04 m. Furthermore, the model's Akaike information criteria (AIC) also decreased from 6314.99 to 5858.75 (Tables 5 and 6).

Table 6. Parameter estimates, standard errors (in parenthesis), variance components, and fit statistics values for the mixed-effects height–diameter model forms.

Components	Mixed-Effects Models		
	M1	**M2**	**M3**
Fixed parameters			
β_0	31.6506 (1.4959)	32.3400 (1.0469)	34.6591 (0.9960)
β_1	23.8515 (1.6557)	25.0679 (1.2465)	28.8907 (1.6301)
Random variance components			
std (u_{0i})	12.1889	5.4512	
std (u_{1i})	11.9283		7.7571
cor (u_{0i}, u_{1i})	0.9380		
σ^2	0.8463	0.9313	0.8122
δ	0.4145	0.4018	0.4704
Model performance			
RMSE (m)	2.6924	2.9144	3.2499
Bias (m)	0.0432	0.0112	−0.0566
AIC	5858.75	6051.30	6316.07

Note: β_0 and β_1 are fixed parameters; std (u_{0i}) and std (u_{1i}) are the standard deviations of the random effects; cor is the correlation between the random effects; σ^2 is the residual variance; δ is the parameter of power-type variance; RMSE, bias, and AIC values are the fit statistics values from the models.

The plot-level predictions follow the observed values closely, providing strong evidence that the best-performing mixed-effects model form (M1) effectively captures the variations in the height–diameter relationship of *Juniperus procera* trees in the Chilimo forest (Figure 3a). This is further evident in the observed versus predicted graph, which illustrates that the model enables precise height predictions (Figure 3b). Moreover, upon examining the standardized residuals graph, we found that there are no indications of a violation of the assumption of homoscedasticity in the residual distribution (Figure 3c). The residuals exhibit a uniform distribution around the zero line, and there is no systematic trend in their distribution.
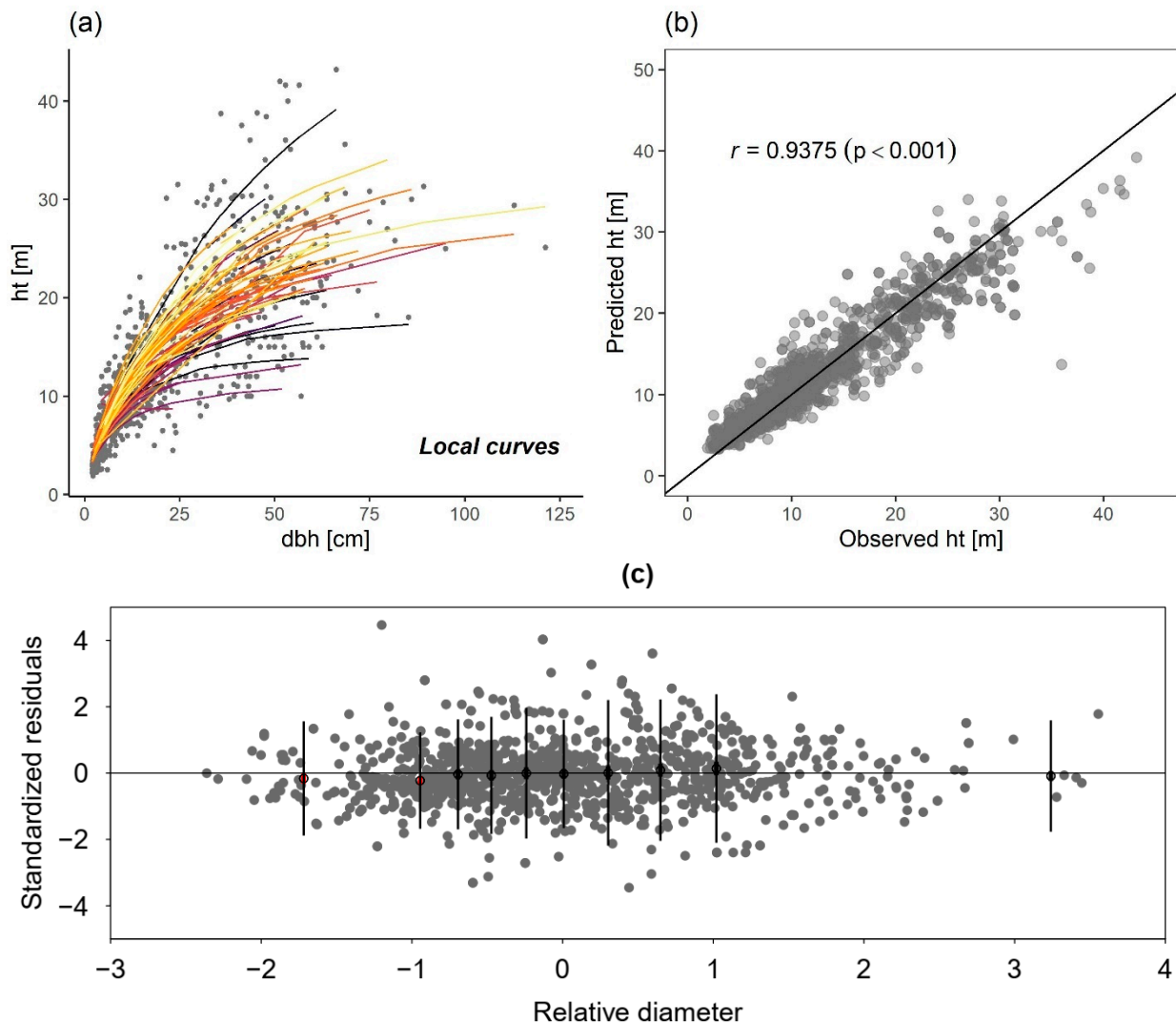
Figure 3. Plot-specific height diameter curves (**a**), observed against predicted height (**b**), and residuals distribution graphs (**c**) of *Juniperus procera* trees, using the mixed-effect model. The lines depicted in (**a**) represent the local curves, where each colored line illustrates a plot-level fit, while the grey dots represent the observed height–diameter data. The grey dots in (**c**) show the standardized residuals; the empty circles show the means of residuals of each relative diameter class. The thin vertical lines show the confidence interval of each observation, while the thick vertical lines show the 95% confidence interval for the class mean. The thick lines that do not cross the horizontal line at $y = 0$ are highlighted in red.

3.3. Generalized Mixed Effects Model

Among the stand variables, stem density (r = −0.38, $p < 0.01$) and quadratic mean diameter (r = 0.26, $p < 0.04$) were correlated with the β_0 and β_1 parameters of the best mixed-effects model (Supplementary Figure S1), respectively. With the incorporation of the specific variables into the best mixed-effects model, a slight improvement (0.11%) was observed in the RMSE values. However, there was no discernable improvement in the AIC, or the model bias values (Tables 6 and 7). The final generalized mixed-effects model resulting from expanding the fixed effects of the best mixed-effects model is as follows:

$$\text{ht}_{ij} = 1.3 + \left((\beta_0 + u_{0i}) \times \text{dbh}_{ij} + \beta_2 \times Dq \right) / \left((\beta_1 + u_{1i}) + \text{dbh}_{ij} + \beta_3 \times \text{tpa} \right) \quad \textbf{M4}$$

Table 7. Parameter estimates, standard error (in parenthesis), and fit statistical values of the best-generalized mixed-effects model.

Components	M4
Fixed parameters	
β_0	28.4695 (1.3859)
β_1	13.4697 (2.1315)
β_2	−1.3338 (0.1496)
β_3	0.1139 (0.0383)
Random variance components	
std (u_{0i})	11.3006
std (u_{1i})	11.1352
cor (u_{0i}, u_{1i})	0.9510
σ^2	0.8019
δ	0.4327
Model performance	
RMSE (m)	2.6921
Bias (m)	0.0724
AIC	5860.53

Note: β_0, β_1, β_2, and β_3 are fixed parameters; std (u_{0i}) and std (u_{1i}) are the standard deviations of the random effects; cor is the correlation between the random effects; σ^2 is the residual variance; δ is the parameter of power-type variance; RMSE, bias, and AIC are the fit statistics values.

The standardized residuals graph of the generalized mixed-effect model (M4) provides no evidence of violating the assumption of homoscedasticity in the residual distribution (Figure 4). The residuals exhibit a uniform distribution around the zero line, and there is no distinct systematic trend in their distribution.
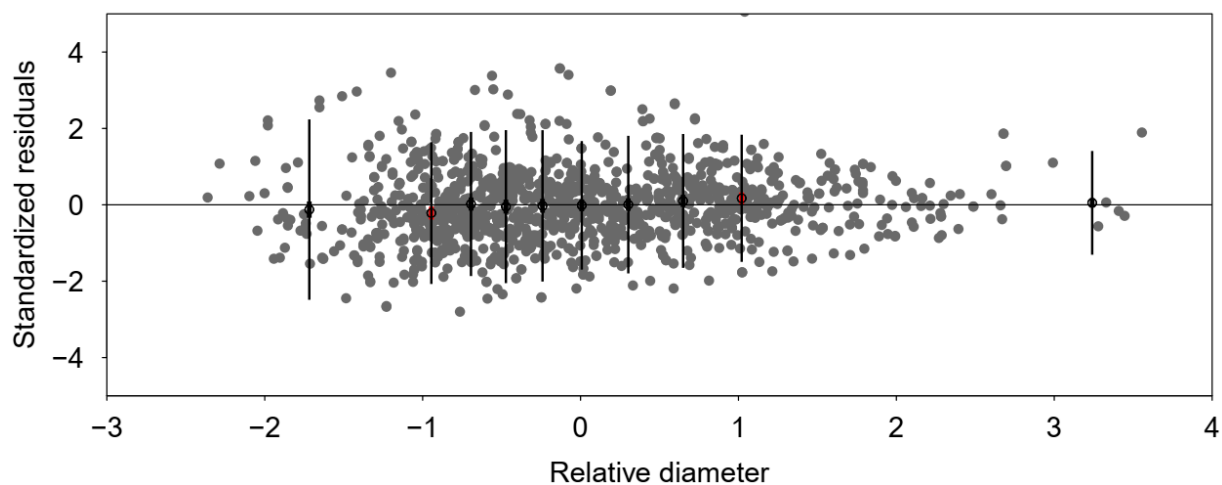
Figure 4. Residuals distribution graph using the generalized mixed-effects model (M4). The grey dots indicate the standardized residuals; the open circles indicate the means of residuals for each diameter class. The thin vertical lines show the confidence interval of each observation, and the thick vertical lines show the 95% confidence interval for the class mean. The thick lines that do not cross the horizontal line at $y = 0$ are highlighted in red.

3.4. Calibration Response

Among the systematic sample selection alternatives (A1–A9), the lowest RMSE value was obtained when utilizing measurements from selected trees with diameters close to the quadratic mean diameter, the smallest diameter, and the largest diameter trees (A6) in each sample plot, utilizing the best mixed-effects model (Table 8). Conversely, utilizing measurements from the smallest diameter trees in each sample plot (A7) consistently produced the highest RMSE values for both models. Overall, the systematic selection alternative (A9) consistently outperformed the random selection alternative (A8) when

utilizing the best mixed-effects model (Figure 5). However, the opposite trend was observed when we utilized the generalized mixed-effects model. Generally, the most effective approach for estimating random effects involved systematically measuring the three largest diameter trees within each plot.

Table 8. The RMSE values from the different tree sample sizes and height predicting strategies.

| No | Subsample | N | Model RMSE | |
			Local	Generalized
A0	The best local model	1215	2.6924	2.6921
A1	Quartiles (1,2,3)	3	2.2320	2.4311
A2	Quartiles (1,2)	2	2.5344	2.9109
A3	Quartiles (1,3)	2	2.2873	2.5345
A4	Quartiles (2,3)	2	2.3376	2.6929
A5	Quartiles (2)	1	2.6680	3.1421
A6	Dq, *dmin*, *dmax*	3	2.1354	2.4517
A7	*dmin*	1	2.9954	3.2069
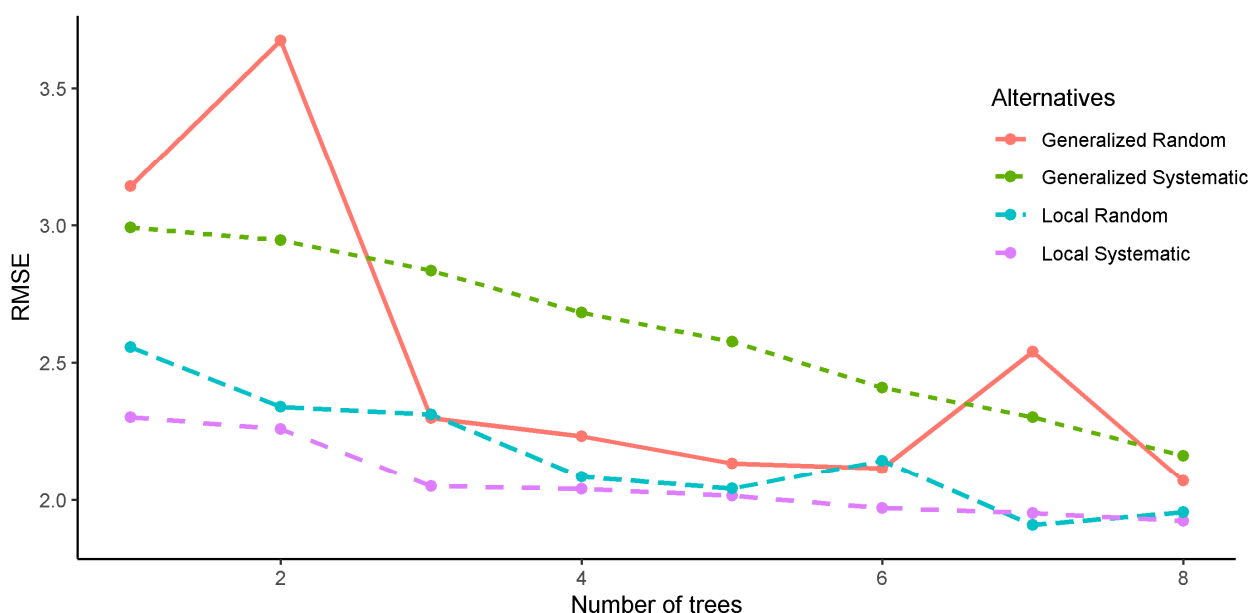
Figure 5. Graphical representation of the RMSE values for the calibration response associated with sampling alternatives A8 and A9. The solid red line represents the results obtained when applying the random tree selection alternative with the generalized mixed-effects model, whereas the green dotted line illustrates the results of the systematic tree selection alternative using the same model. In contrast, the dashed blue line represents the results of using the random tree selection alternative with the local mixed-effects model, whereas the purple dashed line represents the results of using a systematic tree selection alternative for the same model.

4. Discussion

In this study, we developed a height prediction model for *Juniperus procera* trees from dry Afromontane forests of Ethiopia. Among the evaluated local models, the Michaelis–Menten model (M6) showed the best height prediction performance. The addition of random effects on the base model enables capture of the variability in height–diameter relationships amongst the sample plots that were not captured by the base model and provides precise height prediction. We have also shown that the addition of stand-level predictor variables slightly improved the prediction performance of the best local model. Generally, the systematic selection of the three largest-diameter trees from each plot was found to be the best alternative to estimate random effects and predict the height of

trees from a new plot or stand. The results of this study will help researchers and forest managers better understand the height growth pattern and enable them to predict the height of *Juniperus procera* trees from new plots or stands in Afromontane forests.

4.1. Base Model Selection

The Michaelis–Menten model (M6) was first developed to model enzyme kinetics in chemistry [82]; however, it has been widely employed for modeling height–diameter relationships of various tree species (e.g., [31,83–85]). This model has two biologically meaningful parameters that represent the maximum asymptotic height (β_0) a tree can attain, and the steepness (shape) of the curve (β_1) that describes the rate of increase in height [84]. It is an asymptotic model that has been used to estimate heights of trees that lack height measurements during the national forest inventory in Ethiopia [32]. Various studies reported that two-parameter models are generally easier to fit and are quicker to achieve convergence in most situations than the three-parameter models [9,60], which is also supported by this study. Generally, the best base model could be used to determine the average height–diameter relationship of *Juniperus procera* trees in the Chilimo Forest.

4.2. Nonlinear Mixed Effect Model

Utilizing nonlinear mixed-effects models (NLMEM) in height–diameter modeling offers the advantage of incorporating random effects to account for both within-plot and between-plot variability (e.g., [15,86]). The best nonlinear mixed-effects model provided better-fit statistics values than the base model (Tables 5 and 6). This was expected because the random parameters on the mixed-effects models enabled capture of the variations in height–diameter relationships among the sample plots that were not captured by the base model [9]. Huang et al. [87] also stated that the random part of the mixed-effect model allows it to account for plot-level variations due to known and unknown factors, without the need to identify or measure them. This is one of the recognized advantages of using the NLMEM approach.

More specifically, the best mixed-effects model (M1) findings reveal that adding random effects on β_0 and β_1 result in deviations from the population mean, with standard deviations of 12.2 and 11.9 m, respectively (Table 6). These results underscore the variability in the maximum height and curvature of the height–diameter relationship of *J. procera* trees among the sample plots (Table 6). This observed variability may be attributed to differences in soil properties, stand structure, altitude, genetic variability, and competition for resources. Numerous studies have demonstrated that variations in site quality, stem density, elevation, the spatial arrangement of trees within a stand, and microclimatic differences (humidity, temperature, and wind exposure) are primary contributors to variations in height–diameter relationships among different tree species [11,13,88–92]. For example, Feldpausch et al. [11] noted that trees that grew in soils with fewer physical limitations grew taller than those subjected to greater physical limitations. Additionally, van Breugel et al. [93] emphasized the impact of soil fertility and rainfall on the early growth and survival of 49 tropical tree species in Panama. Their study revealed that trees in areas with higher soil fertility and abundant rainfall exhibited greater height and diameter size than trees in regions with lower fertility, highlighting the role of soil fertility in determining tree size. Furthermore, differences in topography can contribute to variations in height–diameter relationships, resulting in taller trees in the valleys compared to ridges in drier areas, and vice versa in wetter regions [94]. In densely populated stands, trees may have to compete more for resources like water, nutrients, and light, which can hinder their growth and lead to significant height variability [25]. Overall, the complex interplay of ecological factors, competition, species diversity, and environmental conditions within a natural forest collectively contribute to the observed differences in height growth patterns among trees.

4.3. The Use of Additional Stand Variables in Height Prediction

The use of additional predictor variables in height–diameter models is a common practice, often used to enhance the accuracy of height prediction (e.g., [15,30,81,86]. This underscores the notion that the variability in height–diameter relationships among trees can be elucidated to some extent by considering additional stand variables. In this study, we observed that the inclusion of Dq (quadratic mean diameter) and stem density slightly improved height prediction performance (Table 6). These additional stand variables reduced the root mean square error (RMSE) by a mere 0.11%. These findings suggest that Dq and stem density may not be significant in determining tree heights. Similar findings were reported by Ciceu et al. [26], who reported a limited impact of stem density on height prediction performance in their research. Tree height is predominantly influenced by individual tree genetics and environmental factors such as light availability and soil fertility, which the evaluated stand variables may not adequately capture. For example, Neophytou et al. [95] examined how genetic variation relates to height growth in Douglas fir trees in various geographic regions. Their findings emphasized a substantial correlation between genetic variation and height growth in these trees, underlying the pivotal role of genetic factors in determining tree height. Likewise, Sertse et al. (2007) also documented the presence of higher genetic variability within the *Juniperus procera* tree population in the Chilimo forest [96].

4.4. Random Effect Estimation and Model Calibration

The main purpose of calibration is to estimate the random effects and perform height prediction for the same tree species from a new plot or stand [15,26]. This requires a prior measurement of diameter, height, predictor variables, and the estimation of random effects. In the calibration process, the local mixed-effect model appeared to be more flexible and appropriate for height prediction than the generalized version, like the previous findings [15,97]. This is evidenced by the fact that the RMSE values were consistently higher for the generalized mixed-effects model than the local mixed-effects model (Figure 5). Furthermore, the calibrated mixed-effect model's simple structure (i.e., without stand variables) makes it a preferable alternative for height prediction to the generalized mixed-effect model [98].

In this study, different sampling alternatives have been identified for estimating the random effects from a new plot or stand and improving height prediction. Generally, the systematic selection of the three largest-diameter trees from each plot (A9) was found to be the best option to estimate random effects and predict the height of trees from a new plot or stand. This is mainly related to the fact that the largest trees' height represents the plot's dominant height and can be used as an additional stand variable for the model-representing site index (a proxy for site productivity), thereby offering additional information for estimating random effects. This is consistent with the findings of Calama and Montero [12], who stated that measuring the height of four trees with larger diameters in each plot was the best sampling alternative for calibration. Results from other studies also showed that using randomly selected trees closest to the second quartiles of the diameter distribution provided the best calibration results [58]. Similarly, Ogana et al. [24] identified that using measurements from four trees, including the largest and smallest diameters per plot, was the most effective calibration alternative for numerous dominant tree species, considering diverse growth conditions, silvicultural practices, and environmental factors in Sweden.

The choice of the sampling alternative depends on the available data for calibration, and the practical application of the model. If the required calibration data are available, the calibrated local mixed-effects model could be used, using the three largest-diameter trees alternative (A9) or the second-best sampling alternative (A6). However, if the calibration data are unavailable, the generalized mixed-effect model (M11) may be the best option because additional stand variables are included in the model. The additional stand variables will enable the model to capture the natural variability among the sample plots. Moreover, if the calibration data and/or the stand variables are not available, the fixed-effects model

(with no random parameters) or the mixed-effects model (random parameters = 0) could be used for tree height prediction [79]. Overall, the three largest-diameter tree measurement alternative (A9) is advantageous, since it requires less sampling effort in terms of cost and time for data collection [19]. The use of the model, along with the proposed sampling alternatives, will ensure high accuracy in height prediction while minimizing the time and cost associated with fieldwork.

In a wider framework of forest management, the localization of the mixed-effects model provides an alternative solution for accurate height predictions that are currently required for total standing volume estimations. In this sense, Van Laar and Akça [99] recommended a minimum sample of 20 to 25 observations per stand to derive accurate growth equations based on statistical approaches. Based on the results of the current study, a small sample comprising three large trees is adequate to estimate the random part of the mixed-effects model and provide reasonable height predictions, minimizing the sampling effort for data collection at the forest stand level.

5. Conclusions

We conclude that the Michaelis–Menten model provided the best height prediction of the height–diameter relationship of the *Juniperus procera* tree among the evaluated local models. Adding quadratic mean diameter and stem density contributed little toward improving the height prediction performance. However, the best mixed-effects model captured the between-plot variation in the height–diameter relationship and provided plot-level height prediction. The fixed effects in the mixed-effects model can be used for the prediction of the mean height of *Juniperus procera* trees for a given diameter in the Chilimo Forest. We also conclude that measuring the three largest-diameter trees is the best sampling alternative for estimating the random effects and predicting the heights of trees from new plots or stands. We believe that the calibrated height–diameter model developed in this study will help researchers and forestry practitioners to reduce costs and time associated with height data collection and improve the accuracy of stand volume and biomass estimation in other Afromontane forests in Ethiopia and elsewhere in Africa.

References

1. Asrat, Z.; Eid, T.; Gobakken, T.; Negash, M. Aboveground tree biomass prediction options for the Dry Afromontane forests in south-central Ethiopia. *For. Ecol. Manag.* **2020**, *473*, 118335. [CrossRef]

2. Guerra-Hernández, J.; Arellano-Pérez, S.; González-Ferreiro, E.; Pascual, A.; Altelarrea, V.S.; Ruiz-González, A.D.; Álvarez-González, J.G.J.F.E. Developing a site index model for P. Pinaster stands in NW Spain by combining bi-temporal ALS data and environmental data. *For. Ecol. Manag.* **2021**, *481*, 118690. [CrossRef]

3. Ruiz-Peinado, R.; Pretzsch, H.; Löf, M.; Heym, M.; Bielak, K.; Aldea, J.; Barbeito, I.; Brazaitis, G.; Drössler, L.; Godvod, K. Mixing effects on Scots pine (*Pinus sylvestris* L.) and Norway spruce (*Picea abies* (L.) Karst.) productivity along a climatic gradient across Europe. *For. Ecol. Manag.* **2021**, *482*, 118834. [CrossRef]

4. Wang, Y.; Zhang, X.; Guo, Z. Estimation of tree height and aboveground biomass of coniferous forests in North China using stereo ZY-3, multispectral Sentinel-2, and DEM data. *Ecol. Indic.* **2021**, *126*, 107645. [CrossRef]

5. Xu, Y.; Li, C.; Sun, Z.; Jiang, L.; Fang, J. Tree height explains stand volume of closed-canopy stands: Evidence from forest inventory data of China. *For. Ecol. Manag.* **2019**, *438*, 51–56. [CrossRef]

6. Holdaway, R.J.; McNeill, S.J.; Mason, N.W.; Carswell, F.E. Propagating uncertainty in plot-based estimates of forest carbon stock and carbon stock change. *Ecosystems* **2014**, *17*, 627–640. [CrossRef]

7. Hunter, M.; Keller, M.; Victoria, D.; Morton, D. Tree height and tropical forest biomass estimation. *Biogeosciences* **2013**, *10*, 8385–8399. [CrossRef]

8. Larjavaara, M.; Muller-Landau, H.C. Measuring tree height: A quantitative comparison of two common field methods in a moist tropical forest. *Methods Ecol. Evol.* **2013**, *4*, 793–801. [CrossRef]

9. Mehtätalo, L.; de-Miguel, S.; Gregoire, T.G. Modeling height-diameter curves for prediction. *Can. J. For. Res.* **2015**, *45*, 826–837. [CrossRef]

10. Imani, G.; Boyemba, F.; Lewis, S.; Nabahungu, N.L.; Calders, K.; Zapfack, L.; Riera, B.; Balegamire, C.; Cuni-Sanchez, A. Height-diameter allometry and above ground biomass in tropical montane forests: Insights from the Albertine Rift in Africa. *PLoS ONE* **2017**, *12*, e0179653. [CrossRef]

11. Feldpausch, T.R.; Banin, L.; Phillips, O.L.; Baker, T.R.; Lewis, S.L.; Quesada, C.A.; Affum-Baffoe, K.; Arets, E.J.; Berry, N.J.; Bird, M. Height-diameter allometry of tropical forest trees. *Biogeosciences* **2011**, *8*, 1081–1106. [CrossRef]

12. Calama, R.; Montero, G. Interregional nonlinear height diameter model with random coefficients for stone pine in Spain. *Can. J. For. Res.* **2004**, *34*, 150–163. [CrossRef]

13. Banin, L.; Feldpausch, T.R.; Phillips, O.L.; Baker, T.R.; Lloyd, J.; Affum-Baffoe, K.; Arets, E.J.; Berry, N.J.; Bradford, M.; Brienen, R.J. What controls tropical forest architecture? Testing environmental, structural, and floristic drivers. *Glob. Ecol. Biogeogr.* **2012**, *21*, 1179–1190. [CrossRef]

14. Sileshi, G.W.; Nath, A.J.; Kuyah, S. Allometric scaling and allocation patterns: Implications for predicting productivity across plant communities. *Front. For. Glob. Chang.* **2023**, *5*, 1084480. [CrossRef]

15. Raptis, D.I.; Kazana, V.; Kazaklis, A.; Stamatiou, C. Mixed-effects height–diameter models for black pine (*Pinus nigra* Arn.) forest management. *Trees* **2021**, *35*, 1167–1183. [CrossRef]

16. Temesgen, H.; Zhang, C.; Zhao, X. Modelling tree height–diameter relationships in multi-species and multi-layered forests: A large observational study from Northeast China. *For. Ecol. Manag.* **2014**, *316*, 78–89. [CrossRef]

17. Temesgen, H.; v Gadow, K. Generalized height–diameter models–an application for major tree species in complex stands of interior British Columbia. *Eur. J. For. Res.* **2004**, *123*, 45–51. [CrossRef]

18. Curtis, R.O. Height-diameter and height-diameter-age equations for second-growth Douglas-fir. *For. Sci.* **1967**, *13*, 365–375.

19. Dorado, F.C.; Diéguez-Aranda, U.; Anta, M.B.; Rodríguez, M.S.; von Gadow, K. A generalized height–diameter model including random components for radiata pine plantations in northwestern Spain. *For. Ecol. Manag.* **2006**, *229*, 202–213. [CrossRef]

20. Ercanli, I. Nonlinear mixed effect models for predicting relationships between total height and diameter of Oriental beech trees in Kestel, Turkey. *Rev. Chapingo Ser. Cienc. For. Del Ambiente* **2015**, *21*, 185–202. [CrossRef]

21. Pinheiro, J.C.; Bates, D.M. Theory and Computational Methods for Linear Mixed-Effects Models. In *Mixed-Effects Models in S and S-PLUS*; Springer: Berlin/Heidelberg, Germany, 2000; pp. 57–96.

22. Ogana, F.N.; Ercanli, I. Modelling height-diameter relationships in complex tropical rain forest ecosystems using deep learning algorithm. *J. For. Res.* **2022**, *33*, 883–898. [CrossRef]

23. Sharma, R.P.; Vacek, Z.; Vacek, S.; Kučera, M. Modelling individual tree height–diameter relationships for multi-layered and multi-species forests in central Europe. *Trees* **2019**, *33*, 103–119. [CrossRef]

24. Ogana, F.N.; Holmström, E.; Sharma, R.P.; Langvall, O.; Nilsson, U. Optimizing height measurement for the long-term forest experiments in Sweden. *For. Ecol. Manag.* **2023**, *532*, 120843. [CrossRef]

25. Gomez-Garcia, E.; Fonseca, T.F.; Crecente-Campo, F.; Almeida, L.R.; Dieguez-Aranda, U.; Huang, S.; Marques, C.P. Height-diameter models for maritime pine in Portugal: A comparison of basic, generalized and mixed-effects models. *Iforest-Biogeosci. For.* **2015**, *9*, 72. [CrossRef]

26. Ciceu, A.; Garcia-Duro, J.; Seceleanu, I.; Badea, O. A generalized nonlinear mixed-effects height–diameter model for Norway spruce in mixed-uneven aged stands. *For. Ecol. Manag.* **2020**, *477*, 118507. [CrossRef]

27. Lima, R.B.d.; Görgens, E.B.; Elias, F.; de Abreu, J.C.; Baia, A.L.; de Oliveira, C.P.; Silva da Silva, D.A.; Batista, A.P.B.; Lima, R.C.; Sotta, E.D. Height-diameter allometry for tropical forest in northern Amazonia. *PLoS ONE* **2021**, *16*, e0255197. [CrossRef] [PubMed]

28. Kearsley, E.; Moonen, P.C.; Hufkens, K.; Doetterl, S.; Lisingo, J.; Boyemba Bosela, F.; Boeckx, P.; Beeckman, H.; Verbeeck, H. Model performance of tree height-diameter relationships in the central Congo Basin. *Ann. For. Sci.* **2017**, *74*, 1–13. [CrossRef]

29. Mugasha, W.; Mauya, E.; Njana, A.; Karlsson, K.; Malimbwi, R.; Ernest, S. Height-diameter allometry for tree species in tanzania mainland. *Int. J. For. Res.* **2019**, *2019*, 4832849. [CrossRef]

30. Ogana, F.N. A mixed-effects height-diameter model for *Gmelina arborea* Roxb stands in Southwest Nigeria. *J. For. Res.* **2022**, *27*, 1–7. [CrossRef]

31. Panzou, G.J.L.; Bocko, Y.E.; Mavoungou, A.Y.; Loumeto, J.-J. Height–diameter allometry in African monodominant forest close to mixed forest. *J. Trop. Ecol.* **2021**, *37*, 98–107. [CrossRef]

32. Sebrala, H.; Abich, A.; Negash, M.; Asrat, Z.; Lojka, B. Tree allometric equations for estimating biomass and volume of Ethiopian forests and establishing a database. *Trees For. People* **2022**, *9*, 100314. [CrossRef]

33. Sisay, K.; Thurnher, C.; Belay, B.; Lindner, G.; Hasenauer, H. Volume and carbon estimates for the forest area of the amhara region in northwestern ethiopia. *Forests* **2017**, *8*, 122. [CrossRef]

34. Asrat, Z.; Eid, T.; Gobakken, T.; Negash, M. Modelling and quantifying tree biometric properties of dry Afromontane forests of south-central Ethiopia. *Trees* **2020**, *34*, 1411–1426. [CrossRef]

35. Tesfaye, M.A.; Gardi, O.; Bekele, T.; Blaser, J. Temporal variation of ecosystem carbon pools along altitudinal gradient and slope: The case of Chilimo dry afromontane natural forest, Central Highlands of Ethiopia. *J. Ecol. Environ. Conserv.* **2019**, *43*, 17. [CrossRef]

36. Soromessa, T.; Kelbessa, E. Diversity and endemicity of Chilimo forest, central Ethiopia. *Biosci. Discov.* **2013**, *4*, 1–4.

37. Tesfaye, M.A.; Bravo, F.; Ruiz-Peinado, R.; Pando, V.; Bravo-Oviedo, A. Impact of changes in land use, species and elevation on soil organic carbon and total nitrogen in Ethiopian Central Highlands. *Geoderma* **2016**, *261*, 70–79. [CrossRef]

38. Mammo, S.; Kebin, Z.; Chimidi, A.; Ibrahim, H. Soil quality analysis for sustainability of forest ecosystem: The case of Chilimo-Gaji Forest, West Shewa Zone, Ethiopia. *J. Environ. Earth Sci.* **2019**, *9*, 1–9.

39. Lemi, T.; Eshete, A.; Seid, G.; Mulugeta, S.; Egeta, D.; Teshome, M. Aboveground Biomass Models for Indigenous Tree Species in the Dry Afromontane Forest, Central Ethiopia. *Int. J. For. Res.* **2023**, *2023*, 4901521. [CrossRef]

40. Duguma, L.A.; Hager, H.; Gruber, M. The community-state forest interaction in Menagesha Suba area, Ethiopia: The challenges and possible solutions. *For. Trees Livelihoods* **2009**, *19*, 111–128. [CrossRef]

41. Friis, I.; Demissew, S.; Breugel, P.V. *Atlas of the Potential Vegetation of Ethiopia*; The Royal Danish Academy of Sciences and Letters: Copenhagen, Denmark, 2010.

42. Mucheye, G.; Yemata, G. Species composition, structure and regeneration status of woody plant species in a dry Afromontane Forest, Northwestern Ethiopia. *Cogent Food Agric.* **2020**, *6*, 1823607. [CrossRef]

43. Ali, F.; Khan, N.; Ali, K.; Khan, M.E.H.; Jones, D.A. Vegetation pattern and regeneration dynamics of the progressively declining Monotheca buxifolia forests in Pakistan: Implications for conservation. *Sustainability* **2022**, *14*, 6111. [CrossRef]

44. Edwards, S.; Tadesse, M.; Hedberg, I. *Flora of Ethiopia and Eritrea, Volume 2, Part 2: Canellaceae to Euphorbiaceae*; The National Herbarium, Addis Ababa, Ethiopia, and Department of Systematic Botany: Uppsala, Switzerland, 1995.

45. Edwards, S.; Tadesse, M.; Demissew, S.; Hedberg, I. *Flora of Ethiopia and Eritrea, Volume 2, Part 1: Magnoliaceae to Flacourtiaceae*; Addis Ababa, Ethiopia and Uppsala, Sweden; The National Herbarium, Addis Ababa University: Addis Ababa, Etiopia, 2000.

46. Hedberg, I.; Hedberg, O.; Edwards, S. *Flora of Ethiopia and Eritrea. Vol. 3, Pittosporaceae to Araliaceae*; National Herbarium, Addis Ababa University: Addis Ababa, Etiopia, 1989.

47. Hedberg, I.; Friis, I.; Edwards, S. *Flora of Ethiopia and Eritrea. Asteraceae Volume 4 Part 2. Ethiopia*; Department of Systematic Botany, Uppsala University: Uppsala, Sweden; National Herbarium, Addis Ababa University: Addis Ababa, Etiopia, 2004.

48. Hedberg, I.; Edwards, S.; Nemomissa, S. *Flora of Ethiopia and Eritrea. Vol. 4. Part 1, Apiaceae to Dipsacaceae*; National Herbarium, Addis Ababa University: Addis Ababa, Etiopia, 2003.

49. Pohjonen, V.; Pukkala, T. Juniperus procera Hocht. ex. Endl. in Ethiopian forestry. *For. Ecol. Manag.* **1992**, *49*, 75–85. [CrossRef]

50. Negash, L.; Kagnew, B. Mechanisms for the successful biological restoration of the threatened African pencilcedar (*Juniperus procera* Hochst. ex. Endl., *Cupressaceae*) in a degraded landscape. *For. Ecol. Manag.* **2013**, *310*, 476–482. [CrossRef]

51. Farjon, A. *Juniperus procera*. The IUCN Red List of Threatened Species 2013: E.T33217A2835242. Available online: https://www.iucnredlist.org/species/33217/2835242 (accessed on 3 April 2023).

52. Orwa, C.; Mutua, A.; Kindt, R.; Jamnadass, R.; Simons, A. *Agroforestree Database: A Tree Reference and Selection Guide, Version 4.0*; World Agroforestry Centre ICRAF: Nairobi, Kenia, 2009.

53. Abrha, H.; Birhane, E.; Hagos, H.; Manaye, A. Predicting suitable habitats of endangered *Juniperus procera* tree under climate change in Northern Ethiopia. *J. Sustain. For.* **2018**, *37*, 842–853. [CrossRef]

54. White, F. The vegetation of Africa, a descriptive memoir to accompany the UNESCO/AETFAT/UNSO vegetation map of Africa. *UNESCO Nat. Resour. Res.* **1983**, *20*, 356.

55. Zeide, B. Analysis of growth equations. *For. Sci.* **1993**, *39*, 594–616. [CrossRef]

56. Huang, S.; Titus, S.J.; Wiens, D.P. Comparison of nonlinear height–diameter functions for major Alberta tree species. *Can. J. For. Res.* **1992**, *22*, 1297–1304. [CrossRef]

57. Mehtatalo, L.; Lappi, J. *Biometry for Forestry and Environmental Data: With Examples in R*; Chapman and Hall/CRC: Boca Raton, FL, USA, 2020.

58. Corral-Rivas, S.; Álvarez-González, J.G.; Crecente-Campo, F.; Corral-Rivas, J.J. Local and generalized height-diameter models with random parameters for mixed, uneven-aged forests in Northwestern Durango, Mexico. *For. Ecosyst.* **2014**, *1*, 6. [CrossRef]

59. Chenge, I.B. Height–diameter relationship of trees in Omo strict nature forest reserve, Nigeria. *Trees For. People* **2021**, *3*, 100051. [CrossRef]

60. Ogana, F.N.; Corral-Rivas, S.; Gorgoso-Varela, J.J. Nonlinear mixed-effect height-diameter model for *Pinus pinaster* ait. and *Pinus radiata* d. Don. *Cerne* **2020**, *26*, 150–161. [CrossRef]

61. R Core Team. *R: A Language and Environment for Statistical Computing*; R Foundation for Statistical Computing: Vienna, Austria, 2020; Volume 1.

62. Zeide, B.J.C.J.o.F.R. Accuracy of equations describing diameter growth. *Can. J. For. Res.* **1989**, *19*, 1283–1286. [CrossRef]

63. Näslund, M. The thinning experiments of the Forest Research Institute in Scots pine stand. *Medd. Från Statens Skogsförsöksanstalt* **1937**, *29*, 1–169.

64. Meyer, H.A. A mathematical expression for height curves. *J. For.* **1940**, *38*, 415–420.

65. Schumacher, F.X. A new growth curve and its application to timber yield studies. *J. For.* **1939**, *37*, 819–820.

66. Bates, D.M.; Watts, D.G. Relative curvature measures of nonlinearity. *J. R. Stat. Soc. Ser. B* **1980**, *42*, 1–16. [CrossRef]

67. Medawar, P.B. The growth, growth energy, and ageing of the chicken's heart. *Proc. R. Soc. Lond. Ser. B-Biol. Sci.* **1940**, *129*, 332–355.

68. Richards, F.J. A flexible growth function for empirical use. *J. Exp. Bot.* **1959**, *10*, 290–301. [CrossRef]

69. Chapman, D.G. Statistical problems in dynamics of exploited fisheries populations. In Proceedings of the 4th Berkeley Symposium on Mathematical Statistics and Probability, Santa Barbara, CA, USA, 20 June–30 July 1960; pp. 153–168.

70. Yang, R.C.; Kozak, A.; Smith, J.H.G. The potential of Weibull-type functions as flexible growth curves. *Can. J. For. Res.* **1978**, *8*, 424–431. [CrossRef]

71. Ratkowsky, D. *Handbook of Nonlinear Regression Models*; Marcel Dekker: New York, NY, USA, 1990.

72. Mulamba, N.; Mock, J. Improvement of yield potential of the ETO blanco maize (*Zea mays* L.) population by breeding for plant traits [Mexico]. *Egypt. J. Genet. Cytol.* **1978**, *7*, 476–490.

73. Özçelik, R.; Cao, Q.V.; Trincado, G.; Göçer, N. Predicting tree height from tree diameter and dominant height using mixed-effects and quantile regression models for two species in Turkey. *For. Ecol. Manag.* **2018**, *419*, 240–248. [CrossRef]

74. Stegmann, G.; Jacobucci, R.; Harring, J.R.; Grimm, K.J. Nonlinear mixed-effects modeling programs in R. *Struct. Equ. Model.* **2018**, *25*, 160–165. [CrossRef]

75. Cui, K.; Wu, X.; Zhang, C.; Zhao, X.; von Gadow, K. Estimating height-diameter relations for structure groups in the natural forests of Northeastern China. *For. Ecol. Manag.* **2022**, *519*, 120298. [CrossRef]

76. Xie, L.; Widagdo, F.R.A.; Dong, L.; Li, F. Modeling height–diameter relationships for mixed-species plantations of Fraxinus mandshurica Rupr. and Larix olgensis Henry in Northeastern China. *Forests* **2020**, *11*, 610. [CrossRef]

77. Zhang, X.; Fu, L.; Sharma, R.P.; He, X.; Zhang, H.; Feng, L.; Zhou, Z. A Nonlinear Mixed-Effects Height-Diameter Model with Interaction Effects of Stand Density and Site Index for *Larix olgensis* in Northeast China. *Forests* **2021**, *12*, 1460. [CrossRef]

78. Pinheiro, J.; Bates, D.M. Nlme: Linear and Nonlinear Mixed Effects Models. R package Version 3.1-161. Available online: https://CRAN.R-project.org/package=nlme (accessed on 12 May 2022).

79. Patrício, M.S.; Dias, C.R.; Nunes, L. Mixed-effects generalized height-diameter model: A tool for forestry management of young sweet chestnut stands. *For. Ecol. Manag.* **2022**, *514*, 120209. [CrossRef]

80. Vonesh, E.; Chinchilli, V.M. *Linear and Nonlinear Models for the Analysis of Repeated Measurements*; CRC Press: Boca Raton, FL, USA, 1997.

81. Camacho, E.A.R.; Rivas, S.C.; Hernández, J.A.L.; Durán, Á.A.C.; Carmona, J.X.; Nagel, J. Generalized height-diameter models with random effects for natural forests of central Mexico. *CERNE* **2022**, *28*, E-103033. [CrossRef]

82. Johnson, K.A.; Goody, R.S. The original Michaelis constant: Translation of the 1913 Michaelis–Menten paper. *Biochemistry* **2011**, *50*, 8264–8269. [CrossRef]

83. Fayolle, A.; Panzou, G.J.L.; Drouet, T.; Swaine, M.D.; Bauwens, S.; Vleminckx, J.; Biwole, A.; Lejeune, P.; Doucet, J.-L. Taller trees, denser stands and greater biomass in semi-deciduous than in evergreen lowland central African forests. *For. Ecol. Manag.* **2016**, *374*, 42–50. [CrossRef]

84. Molto, Q.; Hérault, B.; Boreux, J.-J.; Daullet, M.; Rousteau, A.; Rossi, V. Predicting tree heights for biomass estimates in tropical forests–a test from French Guiana. *Biogeosciences* **2014**, *11*, 3121–3130. [CrossRef]

85. Barbosa, R.I.; Ramirez-Narvaez, P.N.; Fearnside, P.M.; Villacorta, C.D.A.; Carvalho, L.C.d.S. Allometric models to estimate tree height in northern Amazonian ecotone forests. *Acta Amaz.* **2019**, *49*, 81–90. [CrossRef]
86. Bronisz, K.; Mehtätalo, L. Mixed-effects generalized height–diameter model for young silver birch stands on post-agricultural lands. *For. Ecol. Manag.* **2020**, *460*, 117901. [CrossRef]
87. Huang, S.; Wiens, D.P.; Yang, Y.; Meng, S.X.; Vanderschaaf, C.L. Assessing the impacts of species composition, top height and density on individual tree height prediction of quaking aspen in boreal mixedwoods. *For. Ecol. Manag.* **2009**, *258*, 1235–1247. [CrossRef]
88. Sharma, M.; Yin Zhang, S. Height–diameter models using stand characteristics for Pinus banksiana and Picea mariana. *Scand. J. For. Res.* **2004**, *19*, 442–451. [CrossRef]
89. Temesgen, H.; Hann, D.W.; Monleon, V.J. Regional height–diameter equations for major tree species of southwest Oregon. *West. J. Appl. For.* **2007**, *22*, 213–219. [CrossRef]
90. Sullivan, M.J.; Lewis, S.L.; Hubau, W.; Qie, L.; Baker, T.R.; Banin, L.F.; Chave, J.; Cuni-Sanchez, A.; Feldpausch, T.R.; Lopez-Gonzalez, G. Field methods for sampling tree height for tropical forest biomass estimation. *Methods Ecol. Evol.* **2018**, *9*, 1179–1189. [CrossRef]
91. Marshall, A.R.; Willcock, S.; Platts, P.J.; Lovett, J.C.; Balmford, A.; Burgess, N.D.; Latham, J.E.; Munishi, P.K.; Salter, R.; Shirima, D. Measuring and modelling above-ground carbon and tree allometry along a tropical elevation gradient. *Biol. Conserv.* **2012**, *154*, 20–33. [CrossRef]
92. Tian, D.; Jiang, L.; Shahzad, M.K.; He, P.; Wang, J.; Yan, Y. Climate-sensitive tree height-diameter models for mixed forests in Northeastern China. *Agric. For. Meteorol.* **2022**, *326*, 109182. [CrossRef]
93. van Breugel, M.; Hall, J.S.; Craven, D.J.; Gregoire, T.G.; Park, A.; Dent, D.H.; Wishnie, M.H.; Mariscal, E.; Deago, J.; Ibarra, D. Early growth and survival of 49 tropical tree species across sites differing in soil fertility and rainfall in Panama. *For. Ecol. Manag.* **2011**, *261*, 1580–1589. [CrossRef]
94. Detto, M.; Muller-Landau, H.C.; Mascaro, J.; Asner, G.P. Hydrological networks and associated topographic variation as templates for the spatial organization of tropical forest vegetation. *PLoS ONE* **2013**, *8*, e76296. [CrossRef]
95. Neophytou, C.; Weisser, A.-M.; Landwehr, D.; Šeho, M.; Kohnle, U.; Ensminger, I.; Wildhagen, H. Assessing the relationship between height growth and molecular genetic variation in Douglas-fir (*Pseudotsuga menziesii*) provenances. *Eur. J. For. Res.* **2016**, *135*, 465–481. [CrossRef]
96. Sertse, D.; Gailing, O.; Eliades, N.G.; Finkeldey, R. Anthropogenic and natural causes influencing population genetic structure of Juniperus procera Hochst. ex Endl. in the Ethiopian highlands. *Genet. Resour. Crop Evol.* **2011**, *58*, 849–859. [CrossRef]
97. Castaño-Santamaría, J.; Crecente-Campo, F.; Fernández-Martínez, J.L.; Barrio-Anta, M.; Obeso, J.R. Tree height prediction approaches for uneven-aged beech forests in northwestern Spain. *For. Ecol. Manag.* **2013**, *307*, 63–73. [CrossRef]
98. Trincado, G.; VanderSchaaf, C.L.; Burkhart, H.E. Regional mixed-effects height–diameter models for loblolly pine (*Pinus taeda* L.) plantations. *Eur. J. For. Res.* **2007**, *126*, 253–262. [CrossRef]
99. Van Laar, A.; Akça, A. *Forest Mensuration*; Springer Science & Business Media: Berlin/Heidelberg, Germany, 2007; Volume 13.